



Electronic structure and optical properties of prominent phases of TiO₂: First-principles study

SANTOSH SINGH and MADHVENDRA NATH TRIPATHI*

Department of Pure and Applied Physics, Guru Ghasidas Vishwavidyalaya (Central University), Koni, Bilaspur 495 009, India

*Corresponding author. E-mail: ommadhav27@gmail.com

Published online 19 June 2017

Abstract. First-principles study based on density functional theory (DFT) of two prominent phases, the rutile and the anatase phases, of titanium dioxide (TiO₂) are reported within the generalized gradient approximation (GGA). Our calculated band structure shows that there is a significant presence of O-2p and Ti-3d hybridization in the valence bands. These bands are well separated from the conduction bands by a direct band gap value of 1.73 eV in the rutile phase and an indirect band gap value of 2.03 eV in the anatase phase, from Γ to X. Our calculations reproduced the peaks in the conduction and valence band, are in good agreement with experimental observations. Our structural optimization for the rutile and anatase phase led to lattice parameter values of 4.62 Å and 2.99 Å rutile and 3.80 Å and 9.55 Å for anatase for *a* and *c*. The static dielectric values 7.0 and 5.1 for the rutile and anatase phases respectively are in excellent agreement with experimental results. Our calculation of optical properties reveals that maximum value of the transmittance in anatase phase of TiO₂ may be achieved by considering the anisotropic behaviour of the optical spectra in the optical region for transparent conducting application.

Keywords. Optoelectronic; titanium oxide.

PACS Nos 73.61.GA; 78.66

1. Introduction

Improving the optoelectronic properties of the already existing transparent conducting materials as well as searching for new transparent conducting materials are the basic needs for designing next-generation displays and photovoltaic devices [1]. Although ITO (indium tin oxide) is still a principal candidate in transparent conducting electronic devices industry, however, due to shortage and high price of indium, so much effort is being invested in the development of new materials which meet suitable for future challenges. The widely investigated substitutes of ITO are SnO₂, ZnO and TiO₂, have typically an order of magnitude of resistivity bit higher than ITO [2]. Moreover, TiO₂-based materials for transparent conducting oxides (TCO) applications has some advantages over indium-based TCO materials, such as high refractive index, high transmittance in the infrared region and high chemical stability in reducing atmosphere [3].

Generally, in order of abundance, titanium dioxide (TiO₂) occurs in nature in three distinct forms which are rutile, anatase, and brookite in the order of

abundance. The rutile and anatase structures are the most important phases for applications and the rarer mineral brookite is not used commercially. TiO₂ in rutile phase is widely used as a white pigment and opacifier due to its high reflectivity across the visible spectrum whereas the anatase phase finds applications in photo catalysts and nanostructured solar cells [4–7]. Rutile is commonly used in thin film capacitors due to its high dielectric constant. Anatase has excellent optical transmittance in the visible and near-infrared regions because it has wide band gap ranging from 3.00 to 3.10 eV. Their structural, electric and optical properties have been experimentally measured using various methods [8–11]. Recently, Vazquez *et al* developed multifunctional P-doped TiO₂ films [12]. Furthermore, Atanelov *et al* theoretically studied the p element (C,N) codoped rutile TiO₂ [13]. In view of the fact that, tetragonal unit cells of both rutile and anatase phases of TiO₂ show large anisotropic nature [2,14]. Hence, due to larger anisotropy, the optical properties are strongly dependent on the direction of incoming polarized light. When the polarization direction is perpendicular (E_{\perp}) or parallel (E_{\parallel}) to the *c*-axis, a high degree of fine structure exists

in the optical properties [15]. Recently, after taking into consideration of the anisotropy of the crystal structure and the nonparabolicity of the bands, Huey *et al* [2], reported the effective masses of electrons in orthogonal and parallel directions of tetragonal axis of Nb-doped anatase crystal of TiO_2 as a function of carrier concentration and found the concentration range relevant for transparent conducting applications which are also confirmed by other groups [16,17]. Although transmittance (T) is also an important physical parameter for transparent conducting application, even though the effect of anisotropy of crystal on transmittance spectra for both rutile and anatase phases of TiO_2 is not investigated till now. In the present study, we have reported the anisotropy-dependent transmittance spectra of the rutile and anatase phases of TiO_2 . It is obvious that electronic structures need to be accurately studied because they are the starting point for first-principles calculations of other physical and chemical properties. First-principles study based on density functional theory (DFT) of the two prominent phases, rutile and anatase, of TiO_2 are reported within the generalized gradient approximation (GGA).

2. Computational details

The calculations were based on the DFT implemented on CASTEP code using ultrasoft pseudopotential to describe electron–ion interaction and plane-wave expansion of the wave function. The Perdew–Burke–Ernzerhof (PBE) parametrization for the GGA is used to express exchange correlation potential. The plane-wave cut-off energy was set to 380 eV. All the structures were fully optimized until the magnitude of force on each ion became less than 0.001 eV/Å and the computational error was limited to less than 1 meV per unit cell. Transmittance $T(\omega)$ can be calculated from [18]

$$T(\omega) = (1 - R(\omega))e^{-\alpha(\omega)t}. \quad (1)$$

3. Results and discussion

3.1 Structural details and electronic structure

Both rutile and anatase phases of TiO_2 have tetragonal structure. In the rutile unit cell as shown in figure 1, each Ti atom is surrounded by a slightly distorted octahedron of O atoms, oxygen atoms forming a hexagonal closed-packed sublattice with half the octahedral sites being filled with Ti atoms. The titanium and oxygen atoms occupy the Wyckoff positions 2a and 4f. TiO_2 -anatase unit cell contains two TiO_2 units with each Ti ion octahedral coordinated to six O ions. In this phase, the Ti–O octahedron is not regular and the Ti–O bond distances are similar to those in rutile for the long and short bond lengths respectively (see table 1). The titanium and oxygen atoms occupy the Wyckoff positions 4a and 8e. The optimized lattice parameters for the rutile and anatase phases of titanium dioxide within GGA are shown in table 1 which are in good agreement with experimental values. The electronic structures of two prominent phases are studied within GGA parametrization. The band structures of the pure rutile and anatase phases of TiO_2 are shown in figures 2a and 2b respectively. It is observed that rutile structure has a direct band-gap value of 1.73 eV at Γ point whereas anatase has an indirect band-gap value of 2.03 eV from Γ –X path. It is consistent with previous observations [19].

The top valence band in the rutile phase is broader and the lowest conduction band is more localized than the anatase phase. The bottom of the conduction band in the anatase phase is more dispersive than the rutile phase, which is confirmed by the effective mass calculation (see table 2). Therefore, anatase has much better optoelectronic properties than rutile as reported in experimental observations [22]. On the contrary, the top of the valence band in the rutile phase is more dispersive than that of the anatase phase which is clear from band structure shown in figure 2. The partial density of states (PDOS)

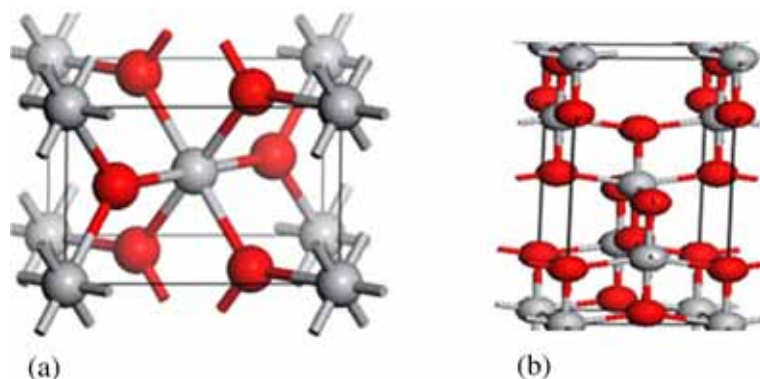


Figure 1. Unit cell structure of (a) rutile and (b) anatase phases of TiO_2 . Red and gray ball indicate O and Ti atoms respectively.

Table 1. Lattice parameters for the rutile and anatase phases of TiO₂.

Crystal type Values	Rutile		Anatase	
	Present	Exp.	Present	Others
Lattice parameter (Å)	$a = 4.58, c = 2.95$	$a = 4.59 [20], c = 2.96$	$a = 3.80, c = 9.55$	$a = 3.78 [20], c = 9.50$
Bond length (Ti–O) (Å)	1.98	1.97 [20]	1.98	1.96 [20]

of both phases are shown in figure 3. It is obvious that main contribution at the top of the valence band comes from O 2p states whereas at the bottom of the conduction band, primarily Ti 3d states are contributing. In rutile and anatase phases of TiO₂, Ti is surrounded by an octahedron of oxygen atoms. So it may be possible that this arrangement of Ti and O atoms permit hybridization between O 2p states and Ti 3d states and due to effective repulsion between them, O 2p states appear on the upper most part of the valence band and enhance the broadness of the valence band. The Ti 3d state around –4 eV in the band structure diagram in both rutile and anatase phases is due to crystal field splitting. The upper conduction band is broader in the anatase phase which may provide more states for optical transitions.

3.2 Optical properties

The imaginary and real parts of dielectric functions for the rutile and anatase phases are shown in figures 4a and 4b respectively. In the rutile phase of TiO₂, the fundamental absorption starts at 2 eV resulting from top of valence band to bottom of conduction band at Γ point. The first transition peak in the imaginary part of the rutile phase occurs at 4 eV due to direct transitions in the vicinity of R and A points. The next transition peak at 7.5 eV is due to the transition between valence band maximum and the Ti 3d states in the conduction band at Γ point. The absorption starts in the anatase phase around 2.0 eV. The first transition peak is similar to rutile but the second peak is less intense than rutile. Contrary to rutile, the imaginary dielectric part becomes zero at 10 eV. The static dielectric value comes from the real part of dielectric function at zero frequency, which are 7.0 for rutile and 5.1 for anatase phases. The dielectric value of rutile is in excellent agreement with the experimental value [23]. The extraordinary ($E \parallel c$) and ordinary ($E \perp c$) components of the absorption coefficient and reflectivity for both the phases are shown in figure 5. In lower energy region, the ordinary component of absorption spectra shows a little blue shift in the rutile phase whereas no shift occurs in the anatase phase, whereas for higher energy region the ordinary component of the anatase phase shows significant blue shift in absorption coefficient compared to its extraordinary component. Similar blue shift is also observed in reflectivity spectra. Further, in lower energy region, particularly below 5 eV, in rutile phase ordinary component of absorption coefficient and reflectivity are slightly smaller than the extraordinary component. On the contrary, both components of the anatase phase have almost the same values of absorption coefficient and reflectivity below 3 eV and larger values are observed above

Table 2. The effective masses of electron and hole (in the unit of m_0) around Γ point for the rutile and anatase phases of TiO_2 .

Phase type	m_h^*			m_e^*		
	$\Gamma - X$	$\Gamma - Z$	$\Gamma - M$	$\Gamma - X$	$\Gamma - Z$	$\Gamma - M$
Rutile	0.54	1.35	0.76	0.59	0.6	1.2
Anatase	0.93	1.62	0.59	0.26	2.22	0.26

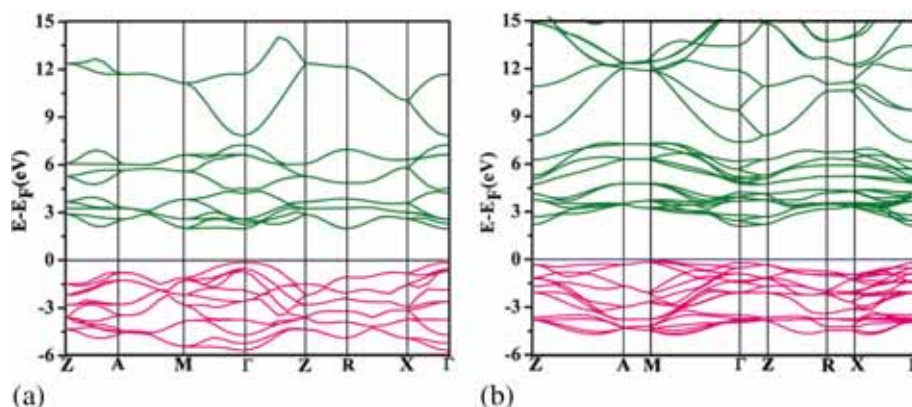


Figure 2. Band structure of (a) rutile and (b) anatase phases of TiO_2 .

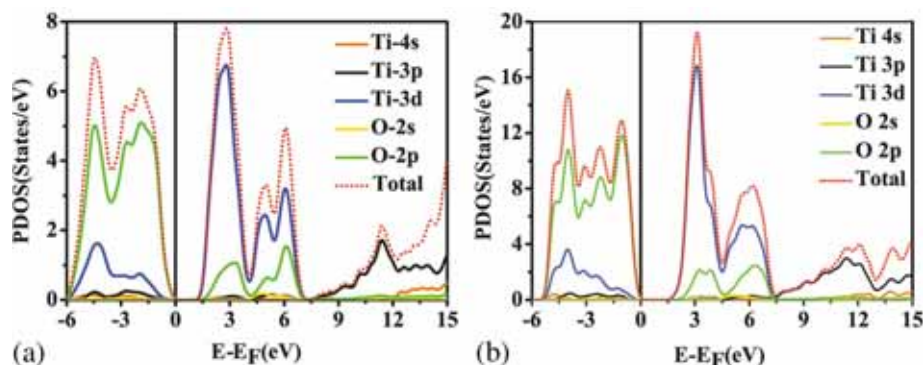


Figure 3. Density of states of (a) rutile and (b) anatase phases of TiO_2 .

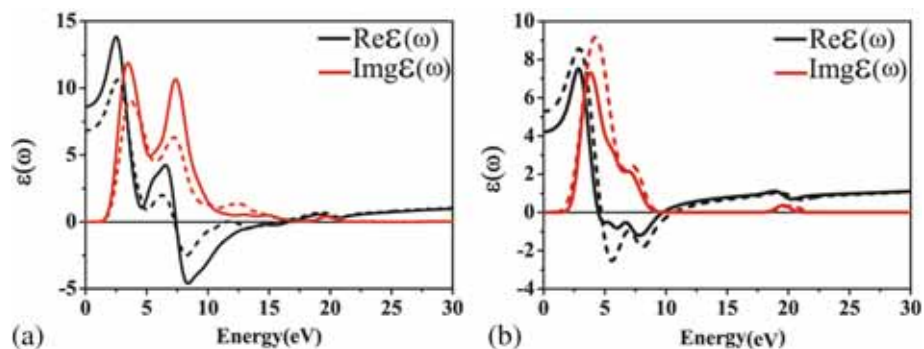


Figure 4. Dielectric functions of (a) rutile and (b) anatase phases. The solid and dashed curves of the same colour represent extraordinary ($E||c$) and ordinary ($E\perp c$) components respectively.

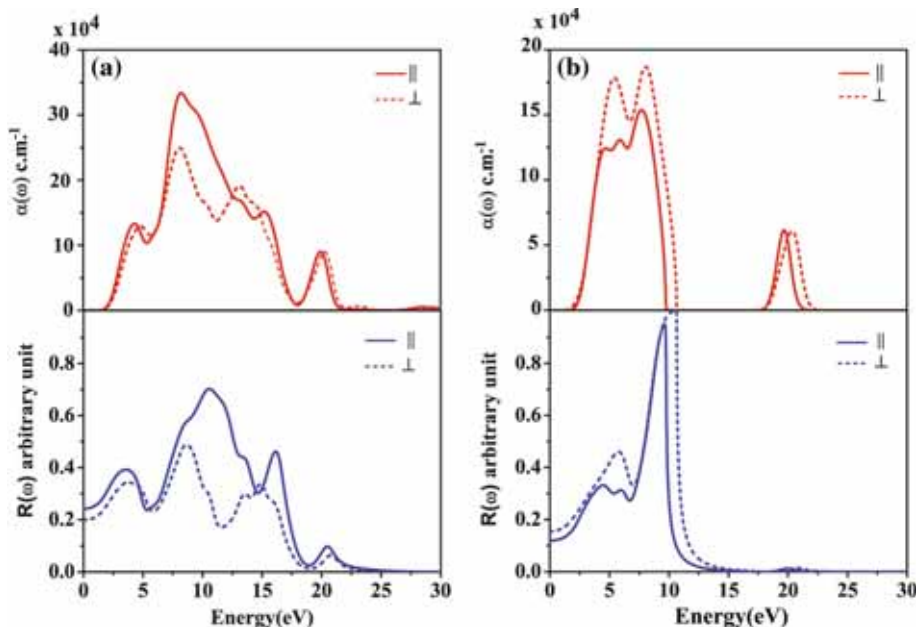


Figure 5. Absorption and reflectivity spectra of (a) rutile and (b) anatase phases of TiO₂. The solid and dashed curves of the same colour represent extraordinary ($E\parallel c$) and ordinary ($E\perp c$) components respectively.

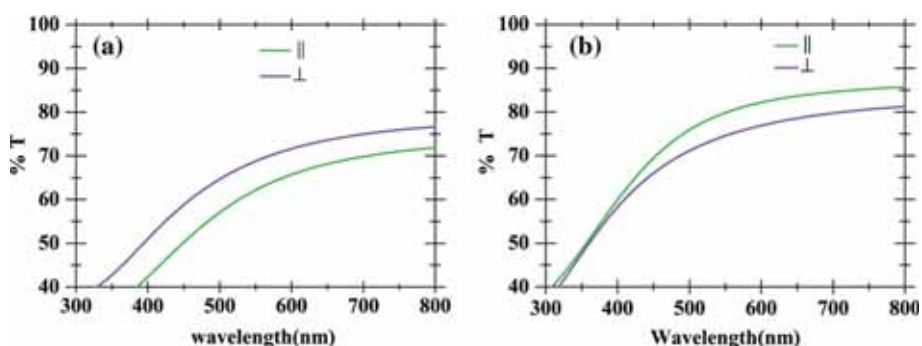


Figure 6. Transmittance spectra of (a) rutile and (b) anatase phases of TiO₂.

3 eV. The larger values of ordinary components in the anatase phase result in the lower value of transmittance as compared to extraordinary component as shown in figure 6. Moreover, overall transmittance of both the phases, shows that rutile phase has lower transmittance than anatase phase. Further, we also observed that the anisotropy present in structural symmetry of the rutile and anatase phases of TiO₂ significantly influences the transmittance spectra of both the phases in the optical region and shows almost 5% difference in transmittance (T) values of extraordinary ($E\parallel c$) and ordinary ($E\perp c$) components of both the phases respectively. In rutile TiO₂, the ordinary ($E\perp c$) components show larger transmittance than the extraordinary component ($E\parallel c$) with a value of almost 80% while in anatase TiO₂, transmittance for the extraordinary component is larger than ordinary component with the value of 85%, and this is clearly visible in figure 6.

4. Conclusion

The electronic structure calculation based on DFT is carried out within GGA parametrization. The optimized lattice parameters are in good agreement with experimental values. The partial density of states shows that top of the valence band is of O 2p type and bottom of the conduction band is of Ti 3d type. The direct band gap is observed in the rutile phase whereas indirect band gap is observed in the anatase phase. The fundamental absorption starts at 2.0 eV from the top of the valence band to the bottom of the conduction band at Γ point. The static dielectric values 7.0 and 5.1 for the rutile and anatase phases are in excellent agreement with experimental results. Moreover, our structural anisotropic-dependent transmittance spectra calculation of the rutile and anatase phases of TiO₂ shows the anisotropic behaviour of the optical

spectra in both phases and reveal that the transmittance of extraordinary component ($E\parallel c$) for the anatase phase is larger than the ordinary component ($E\perp c$) and also greater than the transmittance of extraordinary and ordinary components of the rutile phase of TiO_2 . Henceforth, the maximum value of transmittance in the anatase phase of TiO_2 may be achieved by considering the anisotropic behaviour of the optical spectra in optical region for transparent conducting application.

Acknowledgements

MNT is thankful to UGC-New Delhi for UGC-MRP F.NO. 41-1009/2012 (SR) and SS is thankful to University fellowship. Authors also acknowledge the support from the computational facility of the Department of Pure and Applied Physics, Guru Ghasidas Vishwavidyalaya (Central University).

References

- [1] S Singh and M N Tripathi, *Mater. Res. Express* **3**, 086301 (2016)
- [2] H A Huey, B Aradi, T Frauenheim and P Dek, *Phys. Rev. B* **58**, 155201 (2011)
- [3] Y Bai, I Mora-Sero, F De Angelis, J Bisquert and P Wang, *Chem. Rev.* **114**, 1009510130 (2014)
- [4] S B Zhang, *J. Phys. Condens. Matter* **14**, R881 (2002)
- [5] N Serpone, *J. Phys. Chem. B* **110**, 24287 (2006)
- [6] Shang-Di Mo and W Y Ching, *Phys. Rev. B* **51**, 13023 (1995)
- [7] Y M Lim, J H Jeong, J H An, Y S Jeon, K O Jeon, K S Hwang and B H Kim, *J. Cer. Proc. Res.* **6**, 302 (2005)
- [8] T Umebayashi, T Yamaki, H Itoh and K Asai, *Appl. Phys. Lett.* **81**, 454 (2002)
- [9] A Fujishima and K Honda, *Nature* **238**, 37 (1972)
- [10] M M Islam, T Bredow and A Gerson, *Phys. Rev. B* **76**, 045217 (2007)
- [11] H Fox, K E Newman, W F Schneider and S A Corcelli, *J. Chem. Theory Comput.* **6**, 499 (2010)
- [12] C S Vazquez, N Noor, A Kafizas, R Quesda-Cobra, D O Scahlon, A Taylor, J R Durrant and I P Parkin, *Chem. Mater.* **27**(9), 3234 (2015)
- [13] J Atanelov, C Gruber and P Mohn, *Comput. Mater. Sci.* **98**, 42 (2015)
- [14] K M Glassford and J R Chelikowsky, *Phys. Rev. B* **46**, 1284 (1992)
- [15] M Cardona and G Harbeke, *Phys. Rev. A* **137**, 1467 (1965)
- [16] Y Furubayashi, N Yamada, Y Hirose, Y Yamamoto and M Otani, *J. Appl. Phys.* **101**, 093705 (2007)
- [17] Y Hirose, N Yamada, S Nakao, T Hitosugi, T Shimada and T Hasegawa, *Phys. Rev. B* **79**, 165108 (2009)
- [18] M N Tripathi, K Shida, R Sahara, H Mizusek and Y Kawazoe, *J. Appl. Phys.* **111**, 103110 (2012)
- [19] H Unal, O Glseren, S Ellialtuglu and E Mete, *Phys. Rev. B* **89**, 205127 (2014)
- [20] J K Burdett, T Hughbanks, G J Miller, J W Richerdson Jr. and J V Smith, *J. Am. Chem. Soc.* **109**(12), 3639 (1987)
- [21] J Muscat, V Swamy and N M Harrison, *Phys. Rev. B* **65**, 224112 (2002)
- [22] G L Haller and D E Resasco, *Adv. Catal.* **36**, 173 (1989)
- [23] T A Darvis and K Vedam, *J. Opt. Soc. Am.* **58**, 1446 (1968)